

# Ab initio study of electronic, vibrational and elastic properties of LiInTe<sub>2</sub> and LiTlTe<sub>2</sub> crystals

© Yu.M. Basalae<sup>1,2</sup>, E.B. Duginova<sup>3</sup>, O.G. Basalae<sup>1</sup>

<sup>1</sup> Kemerovo State Medical University,  
650056 Kemerovo, Russia

<sup>2</sup> Russian State Agrarian University Timiryazev Moscow Agricultural Academy,  
127550 Moscow, Russia

<sup>3</sup> Kuzbass State Technical University,  
650000 Kemerovo, Russia

E-mail: ymbas@mail.ru

Received December 17, 2022

Revised January 27, 2023

Accepted January 30, 2023

Using the sublattice method and density functional theory, the electronic structure of a LiTlTe<sub>2</sub> crystal with the chalcopyrite structure was studied for the first time and the equilibrium parameters of the crystal lattice  $a = 6.7526 \text{ \AA}$ ,  $c = 13.3037 \text{ \AA}$ ,  $u(\text{Te}) = 0.2423$  were calculated. It has been established that the valence bands of the LiTlTe<sub>2</sub> crystal and its closest analogue LiInTe<sub>2</sub> actually coincide in topology, and the LiTlTe<sub>2</sub> crystal is a direct-gap semiconductor with a band gap of 0.63 eV and a crystal splitting of 0.04 eV. The partial contributions of the density of states are analyzed and the features of the formation of the valence and conduction bands of LiInTe<sub>2</sub> and LiTlTe<sub>2</sub> crystals due to the contributions of their sublattices are revealed: the structure of the valence bands of both crystals is completely determined by the interaction in the cationic tetrahedra of InTe<sub>4</sub> and TlTe<sub>4</sub>. The vibrational modes and elastic constants are calculated, confirming the stability and mechanical stability of the LiTlTe<sub>2</sub> crystal

**Keywords:** LiInTe<sub>2</sub>, LiTlTe<sub>2</sub>, chalcopyrite, electronic structure, sublattice.

DOI: 10.21883/SC.2023.01.55888.4131

## 1. Introduction

Systematization of structural properties and band gap of triple compounds of type  $A^I M^III X_2^{VI}$  ( $A = \text{Li, Na, K, Rb, Cs}$ ;  $M = \text{Ga, In, Tl}$ ;  $X = \text{S, Se, Te}$ ) was performed in the work [1], where, based on the ratio of ionic radii, the authors proposed to classify these compounds into three structural types, similar to the structures of ZnS, NaCl and TiSe. In particular, it was shown that the compounds LiGaSe<sub>2</sub>, LiGaTe<sub>2</sub>, LiInTe<sub>2</sub>, LiTlS<sub>2</sub>, LiTlSe<sub>2</sub> and LiTlTe<sub>2</sub> must belong to the structural type derived from the structure of sphalerite (ZnS), which was confirmed, for example, for three tellurides in the papers [2–5], in which LiInTe<sub>2</sub> [2], LiAlTe<sub>2</sub> [3] and LiGaTe<sub>2</sub> [4,5] crystals with chalcopyrite structure were synthesized and studied using experimental methods. Among the considered triple compounds of the type Li–III–Te<sub>2</sub> with the structure of chalcopyrite, the crystal LiTlTe<sub>2</sub> has not yet been synthesized and studied, the problem of synthesis and research of which in laboratory conditions is mainly related to the presence in its composition toxic thallium atoms.

The interest in Tl-containing compounds of type I–III–VI<sub>2</sub> with a chalcopyrite structure was associated with the possibility of their use in electro-optical devices. As a rule, the electrical and thermal properties of crystals were studied for this purpose. In particular, in the paper [6], the study of electrical conductivity, thermal EMF and thermal conductivity of the semiconductor AgTlTe<sub>2</sub> in liquid and

solid states was performed where it was also found that the crystal AgTlTe<sub>2</sub> retains the structure of chalcopyrite up to temperature melting point (282°C) and has a positive thermal EMF. The study of the near order in the solid and molten states of the CuTlTe crystal [7] showed the predominant covalent nature of Cu–Te and Tl–Te bonds in both phases with an atom configuration typical of the chalcopyrite structure. Additional interest in Tl-containing compounds with chalcopyrite structure is associated with the search and study of new ideal semimetallic Weyl crystals, which was implemented in the works [8,9] for CuTlSe<sub>2</sub>, AgTlTe<sub>2</sub>, AuTlTe<sub>2</sub> and ZnPbAs<sub>2</sub>.

Special attention should be paid to the work [10], in which the electronic structure was studied using the method of X-ray photoelectron spectroscopy, and the band structure of the LiGaTe<sub>2</sub> crystal was obtained using the methods of the DFT density functional theory. Theoretical and experimental studies successfully complement each other. Using X-ray diffraction analysis, it was possible to estimate the dependence of the lattice parameters on temperature in the range of 303–563 K and to detect a negative thermal expansion along the main axis of the crystal, as well as a predominant thermal expansion in directions perpendicular to it. Using the CASTEP code in the generalized gradient approximation (GGA–PBE), calculations of the band structure, total and partial density of states of the LiGaTe<sub>2</sub> crystal were performed, which, along with experimental data, characterize it as a promising material for use in

the mid-IR range with high anisotropy and low coefficient thermal expansion. The authors of [10] believe that the results obtained for  $\text{LiGaTe}_2$  can be useful for the discovery and study of new IR-optoelectronic multifunctional metal tellurides.

Currently, the problem of studying hypothetical and toxic compounds can be solved using modern *ab initio* calculation methods (*ab initio*), the results of which are comparable in their accuracy with the results of experimental measurements. Such calculations of the energy band structure and dynamics of the crystal lattice for compounds  $\text{LiAlTe}_2$ ,  $\text{LiGaTe}_2$  and  $\text{LiInTe}_2$  with a chalcopyrite structure were carried out within the framework of density functional theory (DFT) in [11,12], where, in general, a good agreement of theoretical and experimental data has been obtained.

The crystal  $\text{LiTlTe}_2$  is hypothetical, as, for example, its isostructural analogues — compounds  $\text{MgSiN}_2$ ,  $\text{MgGeN}_2$  [13] and  $\text{LiMS}_2$  ( $M = \text{B, Al, Ga, In}$ ) [14], which we studied earlier in the framework of density functional theory. As the calculations of [13,14] have shown, the application of the program codes CRYSTAL [15] and Quantum Espresso [16] to the study of the zone structure and dynamics of the lattice of compounds of complex composition, including hypothetical compounds with a chalcopyrite lattice, is a justified and quite effective method of studies. It is safe to say that the method of calculating the electronic and vibrational properties of hypothetical compounds with chalcopyrite structure is well-established and allows for theoretical studies of any isostructural analogues, providing the necessary reliability of the information obtained.

The purpose of this work is modeling and investigation of the energy band structure of a hypothetical  $\text{LiTlTe}_2$  crystal together with its closest really existing and well-studied equivalent  $\text{LiInTe}_2$  with a chalcopyrite structure. This combination of studied items compensates for the absence of any experimental data on the  $\text{LiTlTe}_2$  crystal.

The parameters of the crystal structure of the  $\text{LiTlTe}_2$  crystal necessary for calculations were determined in accordance with the methodology described in [17], which is based on the geometry of the crystal in the chalcopyrite structure, the radii of the atoms and their mutual arrangement. The lattice parameters calculated using formulas from [17] were optimized in the Quantum Espresso code [16] to equilibrium values:  $a = 6.7526 \text{ \AA}$ ,  $c = 13.3037 \text{ \AA}$  ( $\gamma = c/a = 1.970$ ) with anion coordinate  $u(\text{Te}) = 0.2423$ . The parameters of the crystal lattice  $a = 6.308 \text{ \AA}$ ,  $c = 12.385 \text{ \AA}$ ,  $u(\text{Te}) = 0.2382 \text{ \AA}$  for the crystal  $\text{LiInTe}_2$  were taken the same as in the work [9], where they were compared with experimental data  $a = 6.398 \text{ \AA}$ ,  $c = 12.460 \text{ \AA}$ ,  $u(\text{Te}) = 0.2441$  [2, 5].

The coordination environment of each atom in the chalcopyrite structure is equal to four, as a result of which the crystals  $\text{LiInTe}_2$  and  $\text{LiTlTe}_2$  can be represented as a set of „cationic“ (cation in the center)  $\text{LiTe}_4$ ,  $\text{InTe}_4$  ( $\text{LiTe}_4$ ,  $\text{TlTe}_4$ ) and „anionic“ (anion in the center)  $\text{Li}_2\text{TeIn}_2$  ( $\text{Li}_2\text{TeTl}_2$ )

tetrahedra. Te atoms are surrounded by two Li atoms and two In or Tl atoms in anionic tetrahedra. This representation allows for using method of sublattices [18] and considering the participation of atoms of each type in the formation of the zone structure of the corresponding crystal. Calculations demonstrated that the sublattice method allows tracing the genesis of the band structure not only in binary compounds, but also in more complex, for example, triple ion-covalent compounds  $\text{B}_2\text{CN}$ ,  $\text{BC}_2\text{N}$ ,  $\text{BCN}_2$  with a structure similar to the structures of chalcopyrite and antichalcopyrite [18].

In practice, the sublattice method is reduced to calculating the zone structure of the crystal as a single system and additional calculation of zones for the subsystems (sublattices) that make up the crystal: simple, consisting of atoms of the same grade, and complex ones of cation-anion type (cationic tetrahedra).

## 2. Results and discussion

The calculation of the energy band structure of the crystals  $\text{LiInTe}_2$  and  $\text{LiTlTe}_2$  was performed within the framework of the Density Functional Theory (DFTy) using the Quantum Espresso (PWscf) software code [16] and the methods implemented using it on a grid of special points  $16 \times 16 \times 16$ , in the GGA (Generalized Gradient Approximation) approximation using the exchange-correlation function PBE (Perdew-Burke-Ernzerhof) and norm-preserving atomic pseudopotentials generated by the PWscf program. The following configurations of valence electrons were implemented in calculations for crystals  $\text{LiInTe}_2$  and  $\text{LiTlTe}_2$ :  $\text{Li } 2s^1$ ,  $\text{In } 4d^{10}5s^25p^1$ ,  $\text{Tl } 5d^{10}6s^26p^1$ ,  $\text{Te } 5s^25p^4$ . The kinetic energy for both crystals was limited by 40 Ry, and the charge density was limited by 600 Ry, which gives in the decomposition for  $\text{LiInTe}_2$  — 7411, and for  $\text{LiTlTe}_2$  — 8589 flat waves. The electronic structure was calculated across Brillouin zone for the chalcopyrite structure [19], where two directions are the most characteristic and important: 1) along the fourth-order axis  $c$  ( $\Gamma \rightarrow Z$ ) and 2) in a plane perpendicular to it ( $\Gamma \rightarrow X$ ). The origin of the energy scale is combined with the absolute maximum of the valence band of the crystal, coinciding with the last filled state (Fermi level  $E_F$ ).

Comparison of the energy band structures of crystals  $\text{LiInTe}_2$ ,  $\text{LiTlTe}_2$  and their sublattices in Fig. 1 and 2 gives a visual representation of the formation of valence bands from sublattice states of individual atoms that make up compounds.

Due to the fact that the  $d$ -zones of In and Tl atoms in  $\text{LiInTe}_2$  and  $\text{LiTlTe}_2$  crystals are located energetically below the  $s$ -zones of Te atoms (in the region from  $-14$  up to  $-15$  eV relative to  $E_F$ ) and do not actually affect the formation of the valence band, we excluded them from consideration and discussion.

The valence band of the studied crystals  $\text{LiInTe}_2$  and  $\text{LiTlTe}_2$  contains 16 valence electrons (excluding spin and  $d$ -states of In and Tl atoms), which are distributed over

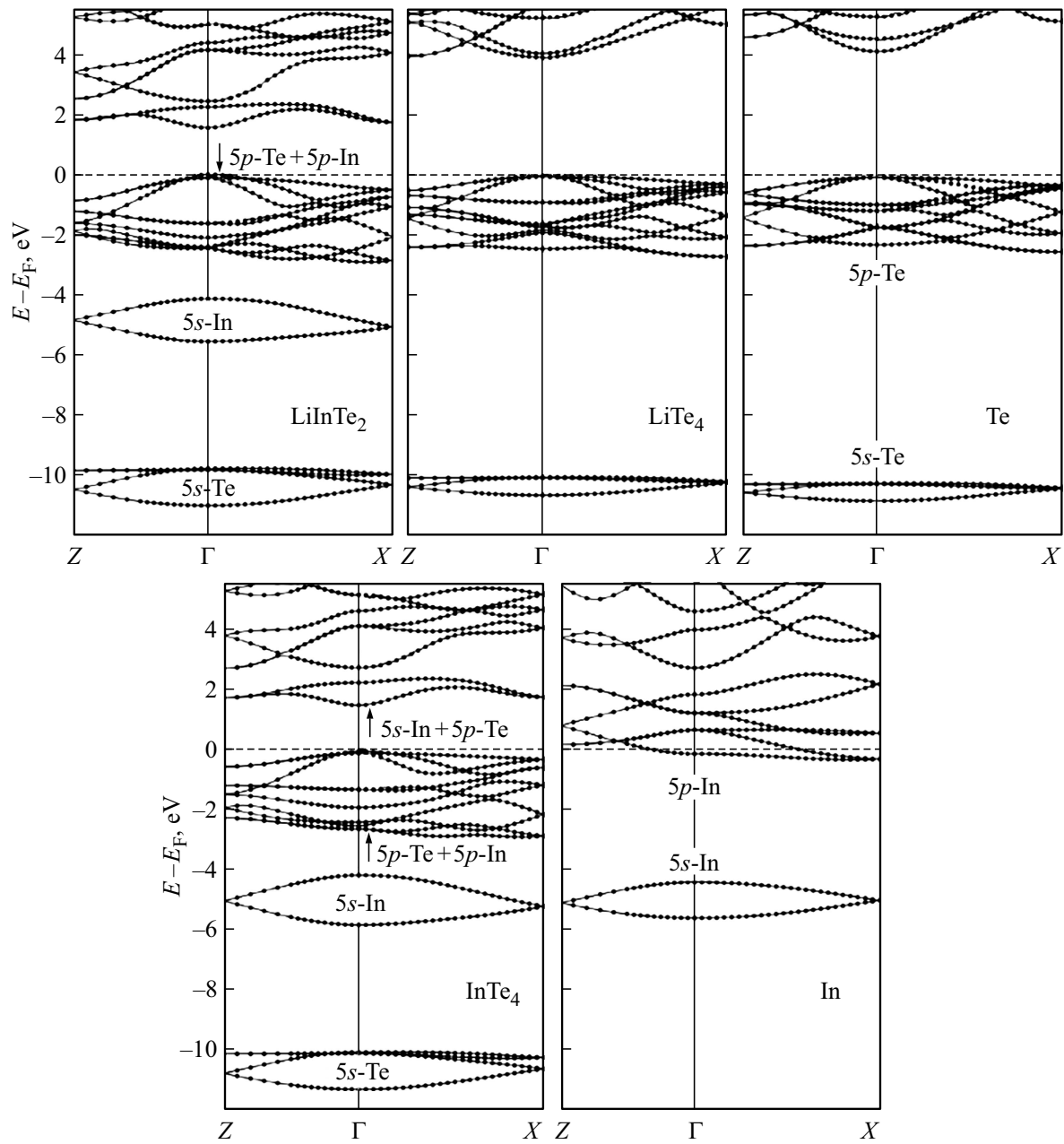


**Figure 1.** The band structure of the crystal  $\text{LiInTe}_2$  and its sublattices.

three allowed zones separated by forbidden sites, which qualitatively coincides with the structure of the valence band of other compounds of the chalcopyrite family [11,19,20].

The margins of the valence band of both crystals are determined by the position of the allowed anion zones:  $5s\text{-Te}$  (lower edge in the range from  $-10$  to  $-11$  eV) and  $5p\text{-Te}$  (upper edge near 0 eV). Thus, the total width of the valence band of crystals  $\text{LiInTe}_2$  and  $\text{LiTlTe}_2$  is  $\sim 11$  eV. It was found that the interaction of anions with cations of different grades leads to the following unequal results. For example, the presence of Li atoms, namely their  $2s$ -states, does not directly affect either the band gap width or the crystal energy levels, but plays an important role

in stabilizing the crystal structure by forming a chemical bond in cationic tetrahedra  $\text{LiTe}_4$ , which does not actually change the band structure formed by a sublattice of Te atoms (see Fig. 1 and 2). As can be seen from the figures, the structure of the valence bands of crystals  $\text{LiInTe}_2$  and  $\text{LiTlTe}_2$  is completely determined by the interaction in cation tetrahedra  $\text{InTe}_4$  and  $\text{TlTe}_4$ , respectively. The interaction of atoms on the In–Te and Tl–Te bonds leads to an increase in the dispersion (broadening) of the  $s$ -zones of atoms in cation tetrahedra  $\text{InTe}_4$ ,  $\text{TlTe}_4$  and, respectively, in crystals, which is typical for the formation of predominantly covalent bonds. The Li–Te chemical bonds in  $\text{LiTe}_4$  tetrahedra are essentially ionic,

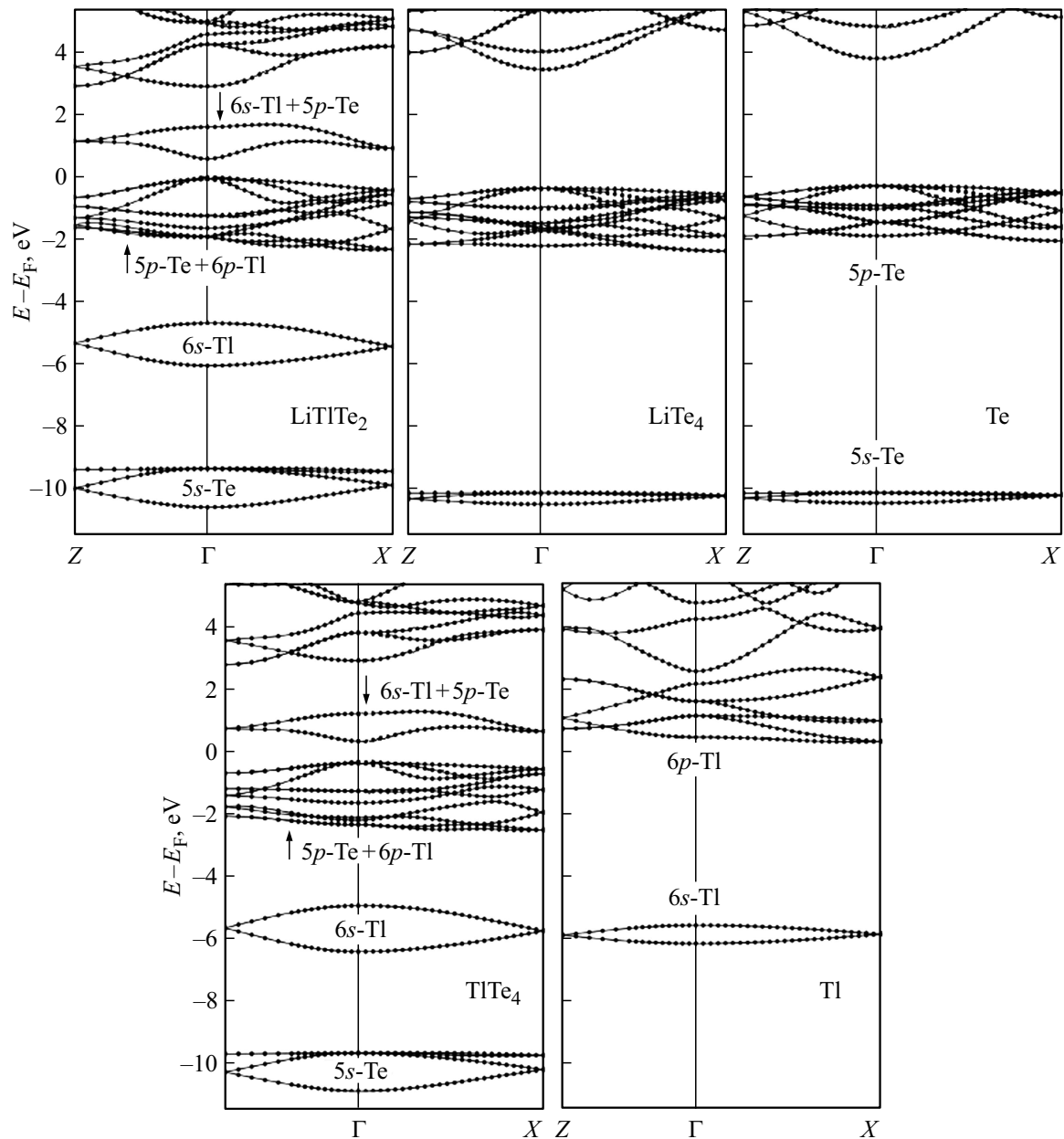


**Figure 2.** The band structure of the  $\text{LiTlTe}_2$  crystal and its sublattices.

which is confirmed experimentally and by calculations by other authors, in particular for  $\text{LiMX}_2$  crystals ( $M = \text{In, Ga}$ ;  $X = \text{S, Se, Te}$ ) [21–24].

The allowed zone in the range from  $-4$  to  $-6$  eV crystals of  $\text{LiInTe}_2$  and  $\text{LiTlTe}_2$  contains mainly contributions of  $s$ -states of elements III group ( $5s\text{-In}$  or  $6s\text{-Tl}$ ) and, as can be traced in Figs. 1 and 2, is due to the formation of bonds  $\text{In-Te}$  and  $\text{Tl-Te}$  in cation tetrahedra  $\text{InTe}_4$ ,  $\text{TlTe}_4$ .

The absolute maximum of the valence band and the minimum of the conduction band of the  $\text{LiTlTe}_2$  crystal are located in the center of the Brillouin zone (point  $\Gamma$ ) and are separated by a straight band gap  $E_g = E_{17}(\Gamma) - E_{16}(\Gamma)$ , equal to 1.66 ( $\text{LiInTe}_2$ ) and 0.63 ( $\text{LiTlTe}_2$ ) eV. The calculated value of  $E_g = 1.66$  eV agrees well with the

experimental value of  $E_g = 1.5$  eV, which was obtained for  $\text{LiInTe}_2$  as a result of studying its optical properties [4]. This result was used in the discussion and generalization of the properties of the group of isoelectronic analogues  $\text{LiMX}_2$  ( $M = \text{In, Ga}$ ;  $X = \text{S, Se, Te}$ ) [21].

Atoms of different grades in cationic sublattices (Li and In (or Tl)) of  $\text{LiInTe}_2$  and  $\text{LiTlTe}_2$  crystals with chalcopyrite structure have different radii, which determines the sizes of  $\text{LiTe}_4$  and  $\text{InTe}_4$  tetrahedra (or  $\text{TlTe}_4$ ), which affect the tetragonal compression of the lattice  $\gamma = c/a = 1.947 < 2.0$  ( $\text{LiInTe}_2$ ),  $\gamma = 1.970 < 2.0$  ( $\text{LiTlTe}_2$ ) and lead to crystal splitting of the vertex of the valence band  $\Delta = E_{16}(\Gamma_{4V}) - E_{15}(\Gamma_{5V})$  by the amount of 0.07 ( $\text{LiInTe}_2$ ) and 0.04 ( $\text{LiTlTe}_2$ ) eV.

The lower unoccupied crystal orbital containing the minimum of the conduction band in the range from 0 to 2.5 eV of both  $\text{LiInTe}_2$  and  $\text{LiTlTe}_2$  crystals is formed mainly from the anti-binding orbitals  $5s$ -In (or  $6s$ -Tl) and  $5p$ -Te. Similar results were obtained from the first principles for the selenide group  $\text{LiAlSe}_2$ ,  $\text{LiGaSe}_2$ ,  $\text{LiInSe}_2$  with a structure derived from the wurtzite structure [24].

Figures 3 and 4 show the total and partial densities of the  $N(E)$  states of the crystals  $\text{LiInTe}_2$  and  $\text{LiTlTe}_2$ . In general, the contributions of the states of individual atoms that make up both crystals give a typical summary picture for the complete crystalline  $N(E)$  valence band of similar tetragonal compounds with the structure of chalcopyrite [14]. The observed main differences in the graphs of  $N(E)$  are obviously determined by the different contributions of Tl and In atoms.

Calculations of the band structure and analysis of partial contributions of the density of states, in combination with the sublattice method, allow studying in detail the structure of not only the valence band, but also the lower part of the conduction band of crystals  $\text{LiInTe}_2$  and  $\text{LiTlTe}_2$ . In particular, it was found that the contributions of the  $p$ -states of Te and In (or Tl) atoms predominate at the vertex of the valence band of both crystals. The contributions of  $s$ -states of In (or Tl) atoms predominate, as well as  $p$ -states of Te atoms and small contributions of  $p$ -states of Li and In (or Tl) atoms near the bottom of the conduction band. These results are well aligned with the data obtained using the WIEN2k code for orthorhombic crystals  $\text{LiGaS}_2$  and  $\text{LiGaSe}_2$  [23], where based on the analysis of partial contributions  $N(E)$  similar contributions of the states of anions (S and Se atoms) and cations (Li and Ga atoms) were established.

Basic information about the chemical bond in a crystal can be obtained from calculating the charge distribution density of valence electrons  $\rho(\mathbf{r})$ . The most obvious is the deformation density of the charge distribution  $\Delta\rho$ , obtained from the crystalline  $\rho(\mathbf{r})$  by subtracting the distribution density for individual non-excited and non-interacting atoms. Then only that part of the charge density that determines the interaction between atoms in the crystal remains on the  $\Delta\rho$  maps. The deformation density  $\Delta\rho$  presented on the map for the  $\text{LiTlTe}_2$  crystal (Fig. 5) shows the presence of charge maxima in the form of closed contours  $\Delta\rho$  on the Li–Te and Tl–Te bonds (covalent component). The Tl–Te bond is predominantly covalent, whereas the Li–Te bond is predominantly ionic, which confirms the position of the charge maximum, which is significantly displaced from the bond center towards the anion. A similar pattern of charge density distribution of valence electrons is observed in the crystal  $\text{LiInTe}_2$  [12,25].

Since the  $\text{LiTlTe}_2$  crystal is hypothetical, to confirm the possibility of its real existence, it is enough to calculate the phonon spectrum and make sure that there are no negative frequencies in it, as well as to find the values of elastic constants and elastic modulus that must satisfy certain conditions.

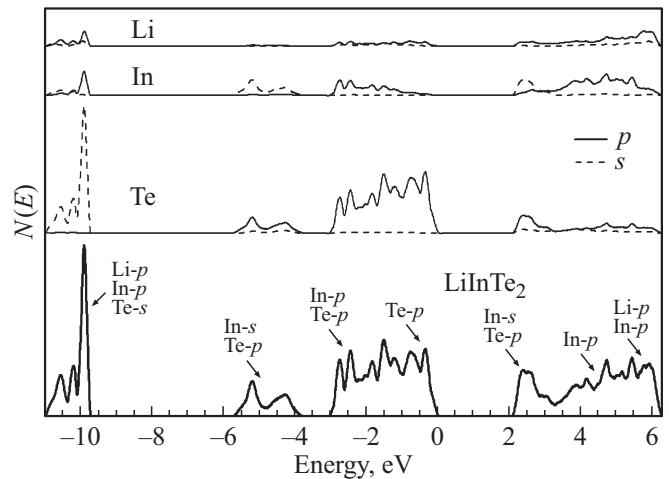


**Figure 3.** The density of states of the crystal  $\text{LiInTe}_2$  and atomic sublattices.

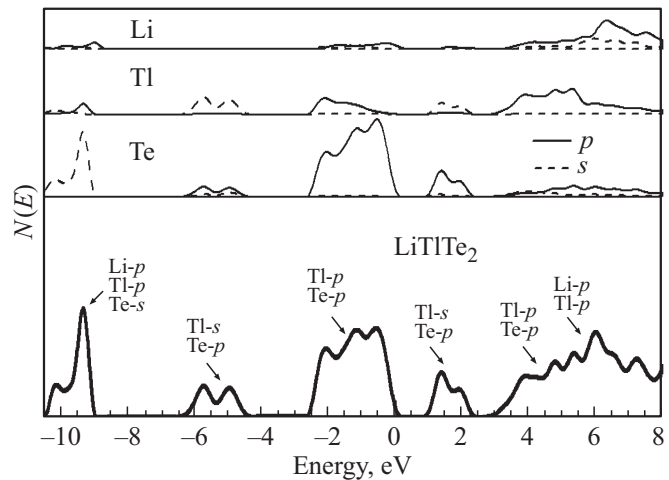


**Figure 4.** The density of states of the crystal  $\text{LiTlTe}_2$  and atomic sublattices.

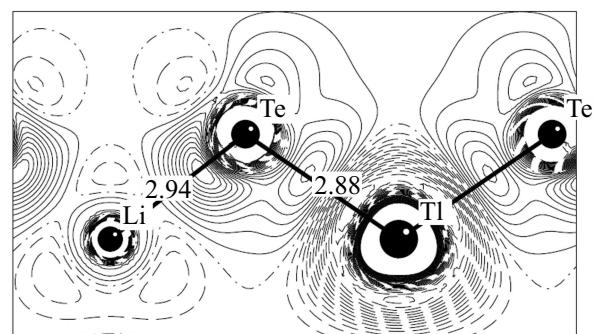


**Figure 5.** Distribution of deformation density in crystal  $\text{LiTlTe}_2$ .

The vibrational spectrum of any crystal consists of infrared (IR) modes and Raman scattering modes, which constitute their „characteristic feature“ — a complete and specific characteristic. The two formula units of crystals

**Table 1.** Frequencies of optical vibrations of crystals LiInTe<sub>2</sub> and LiTlTe<sub>2</sub>

	$\Gamma_1$	$\Gamma_2$	$\Gamma_3$	$\Gamma_4$ TO/LO	$\Gamma_5$ TO/LO
LiInTe <sub>2</sub> [11]	116	91, 132	67, 166, 351	59/63, 163/178, 341/349	38/38, 60/61, 167/168, 169/180, 329/330, 334/347
LiTlTe <sub>2</sub>	104	74, 129	60, 138, 250	53/61, 143/148, 227/250	43/43, 54/56, 135/141, 143/149, 212/213, 233/260

**Table 2.** Elastic constants and the all-round compression modulus ( $B$ ) of crystals LiInTe<sub>2</sub> and LiTlTe<sub>2</sub>

	$C_{11}$	$C_{12}$	$C_{13}$	$C_{33}$	$C_{44}$	$C_{66}$	$B$
LiInTe <sub>2</sub> [11]	37.1	22.1	25.3	42.6	16.6	14.0	29
LiTlTe <sub>2</sub>	38.0	30.6	30.8	47.9	9.9	13.0	34

LiInTe<sub>2</sub> and LiTlTe<sub>2</sub> contain 8 atoms, which, taking into account the symmetry for the chalcopyrite structure, gives a spectrum of lattice vibrations of 24 vibrational modes, including 21 optical and 3 acoustic. The center of the Brillouin zone (the point  $\Gamma$ ) contains the necessary information about the vibrational properties of the crystal and has a certain set of normal vibrations. The spectrum of optical vibrations of LiInTe<sub>2</sub> and LiTlTe<sub>2</sub> crystals in the chalcopyrite structure is represented as the decomposition:  $\Gamma_{\text{opt}} = A_1 + 2A_2 + 3B_1 + 3B_2 + 6E$ . Three acoustic modes ( $B_2$  and  $E$ ) are excluded here and irreducible representations typical of chalcopyrite symmetry are given:  $A_1(\Gamma_1)$ ,  $A_2(\Gamma_2)$ ,  $B_1(\Gamma_3)$ ,  $B_2(\Gamma_4)$  — single and  $E(\Gamma_5)$  — two-to-one representation. All modes (except  $A_2$ ) are active in the Raman spectra of LiInTe<sub>2</sub> and LiTlTe<sub>2</sub> crystals with chalcopyrite structure. The calculated vibrational modes of the crystals LiInTe<sub>2</sub> and LiTlTe<sub>2</sub> are presented in Table 1.

According to the group-theoretic analysis the oscillations with symmetry  $A_1(\Gamma_1)$  and  $A_2(\Gamma_2)$  in both crystals LiInTe<sub>2</sub> and LiTlTe<sub>2</sub> comprise exclusively vibrations of Te atoms. Frequencies with symmetry  $B_1(\Gamma_3)$  include vibrations of atoms in both cationic sublattices of the chalcopyrite lattice (Li and In; Li and Tl), which occur in antiphase along the main axis of symmetry of the crystal ( $c \parallel z$  axis), while Te anions are displaced in a plane perpendicular to this axis. Optical frequencies with symmetry  $B_2(\Gamma_4)$  contain vibrations of Li–Te and Tl–Te bonds or Li–Te and In–Te, in which cations are displaced only along the  $c \parallel z$  axis, and anions oscillate in planes containing this axis. For frequencies with symmetry  $E$ , the displacement of cations is characteristic only in planes perpendicular to the  $c \parallel z$  axis, anions oscillate in planes containing the main axis.

Modes with symmetry  $B_2$  and  $E$  are active and polar in the IR and RAMAN spectra, where they are split into longitudinal (LO) and transverse (TO) components.

The calculated elastic constants of the hypothetical LiTlTe<sub>2</sub> crystal satisfy the Born mechanical stability conditions for tetragonal compounds (Table. 2) the same as for its real equivalent LiInTe<sub>2</sub> [11]: all diagonal elements of the elastic constant matrix are positive  $C_{ii} > 0$ ; the ratios  $C_{11} > C_{12}$ ,  $C_{11}C_{33} > C_{13}^2$  and  $(C_{11} + C_{12})C_{33} > 2C_{13}^2$  are met. The Young's modulus  $E = 22$  GPa, the shear modulus  $G = 8$  GPa, the all-round compression modulus  $B = 34$  GPa and the Poisson's ratio  $\nu = 0.39$  were calculated based on elastic constants for the LiTlTe<sub>2</sub> crystal. From the ratios of compression and shear modules  $B/G = 4.25$  and  $G/B = 0.24$ , it follows that the LiTlTe<sub>2</sub> crystal is a plastic material ( $G/B < 0.5$ ), with high strength, since the value of its Poisson's ratio is close to  $\nu = 0.5$ , corresponding to a mechanically incompressible material.

Microhardness of the LiTlTe<sub>2</sub> ( $H$ , GPa) crystal, calculated using the empirical formula  $H = 0.92 \cdot (G/B)^{1.137} G^{0.708}$  [20], is equal to 0.8 GPa, which indicates its low hardness.

### 3. Conclusion

The stability and mechanical stability of the LiTlTe<sub>2</sub> crystal were established as a result of calculating the equilibrium parameters of the crystal lattice, vibrational frequencies and elastic constants, which determines the possibility of its real existence in the chalcopyrite structure, similar to the real isostructural equivalent of LiInTe<sub>2</sub>. The application of the sublattice method allowed for obtaining the necessary information about the formation of the energy band structure of crystals LiInTe<sub>2</sub> and LiTlTe<sub>2</sub> from sublattice states of cation tetrahedra InTe<sub>4</sub> and TlTe<sub>4</sub>, the study of which in the combination with tetrahedra LiTe<sub>4</sub> provides a visual picture of this process. As a result of calculations, it was found that the LiTlTe<sub>2</sub> crystal is a straight-band semiconductor with a narrow band gap, whose physical properties are similar to those of LiInTe<sub>2</sub>.

### Conflict of interest

The authors declare that they have no conflict of interest.

### References

- [1] Z.Z. Kish, E.Yu. Peresh, V.B. Lazarev, E.E. Semrad. Inorg. Mater., **23**, 697 (1987).
- [2] W. Hönl, G. Kühn, H. Neumann. Z. Anorg. Allgem. Chem., **532**, 150 (1986).
- [3] J. Kim, T. Hughbanks. Inorg. Chem., **39**, 3092 (2000).
- [4] L. Isaenko, P. Krinitsin, V. Vedenyapin, A. Yelisseyev, A. Merkulov, J.J. Zondy, V. Petrov. Cryst. Growth Des., **5**, 1325 (2005).
- [5] L. Isaenko, I. Vasilyeva, A. Merkulov, A. Yelisseyev, S. Lobanov. J. Cryst. Growth, **275**, 217 (2005).
- [6] N. Abdelmohsen, H.H.A. Labib, A.H. Abou El Ela, S. Elsayed. Appl. Phys. A, **48**, 251 (1989).
- [7] O. Uemura, T. Akai, Y. Kameda, T. Satow. Phys. Status Solidi A, **112**, 467 (1989).

- [8] J. Ruan, S.-K. Jian, D. Zhang, H. Yao, H. Zhang, S.-C. Zhang, D. Xing. *Phys. Rev. Lett.*, **116**, 226801 (2016).
- [9] W. Feng, D. Xiao, J. Ding, Y. Yao. *Phys. Rev. Lett.*, **106**, 016402 (2011).
- [10] V.V. Atuchin, F. Liang, S. Grazhdannikov, L.I. Isaenko, P.G. Krinitsin, M.S. Molokeev, I.P. Prosvirin, X. Jiang, Z. Lin. *RSC Advances*, **8**, 9946 (2018).
- [11] A.V. Kosobutsky, Yu.M. Basalaev, A.S. Poplavnoi. *Phys. Status Solidi B*, **246**, 364 (2009).
- [12] Yu.M. Basalaev, Yu.N. Zhuravlev, E.B. Kitova, A.S. Poplavnoi. *J. Struct. Chem.*, **48**, 1001 (2007).
- [13] Y.M. Basalaev, P.V. Demushin. *J. Struct. Chem.*, **51**, 1191 (2010).
- [14] Yu.M. Basalaev, E.V. Duginov, E.B. Duginova. *Uspekhi sovremennogo estestvoznaniya*, **11** (2), 199 (2018) (in Russian).
- [15] R. Dovesi, A. Erba, R. Orlando, C. Zicovich-Wilson, B. Civaleri, L. Maschio, M. Rerat, S. Casassa, J. Baima, S. Salustro, B. Kirtman. *Comput. Mol. Sci.*, **8**, e1360 (2018).
- [16] S. Baroni, S. de Gironcoli, A. Dal Corso, P. Giannozzi. *Rev. Mod. Phys.*, **73**, 515 (2001).
- [17] J.E. Jaffe, A. Zunger. *Phys. Rev. B*, **29**, 1882 (1984).
- [18] Y.M. Basalaev. *J. Struct. Chem.*, **57**, 8 (2016).
- [19] W. Setyawan, S. Curtarolo. *Comput. Mater. Sci.*, **49**, 299 (2010).
- [20] Y. Tian, B. Xu, Z. Zhao. *Int. J. Refract. Met. Hard Mater.*, **33**, 93 (2012).
- [21] L. Isaenko, A. Yelisseyev, S. Lobanov, P.G. Krinitsin, V. Petrov, J.-J. Zondy. *J. Non-Cryst. Sol.*, **352**, 2439 (2006).
- [22] L. Bai, Z.S. Lin, Z.Z. Wang, C.T. Chen. *J. Appl. Phys.*, **103**, 083111 (2008).
- [23] A.H. Reshak, S. Auluck, I.V. Kityk, Y. Al-Douri. *Appl. Phys. A*, **94**, 315 (2009).
- [24] L.-H. Li, J.-Q. Li, L.-M. Wu. *J. Solid State Chem.*, **181**, 2462 (2008).
- [25] C.-G. Ma, M.G. Brik. *Solid State Commun.*, **203**, 69 (2015).

*Translated by A.Akhtyamov*